

# High-power mid-infrared pulse MgO:PPLN optical parametric oscillator pumped by linearly polarized Yb-doped all-fiber laser

Yang He<sup>a</sup>, Yanhui Ji<sup>a,b</sup>, Haohua Wan<sup>a,b</sup>, Deyang Yu<sup>a</sup>, Kuo Zhang<sup>a</sup>, Qikun Pan<sup>a</sup>, Junjie Sun<sup>a,b</sup>, Yi Chen<sup>a</sup>, Fei Chen<sup>a,\*</sup>

<sup>a</sup> State Key Laboratory of Laser Interaction with Matter, Changchun Institute of Optics, Fine Mechanics and Physics, Chinese Academy of Sciences, 3888 Dongnanhu Road, Changchun Jilin 130033, China

<sup>b</sup> University of Chinese Academy of Sciences, Beijing 100049, China

## ARTICLE INFO

### Keywords:

Optical parametric oscillator  
MgO:PPLN  
Mid-infrared  
Yb-doped fiber laser

## ABSTRACT

We present a MgO:PPLN-based optical parametric oscillator (OPO) pumped by all-fiber Yb-doped fiber laser (YDFL). The performances of the linearly polarized YDFL are first investigated. A maximum power of 79.1 W at 1064.1 nm is obtained with the repetition rate of 300 kHz and pulse width of 200 ns. Then we examine the dependence of OPO characteristics on the pump repetition rate, pulse width, and waist diameter. By optimizing these factors, we report a maximum mid-infrared (MIR) power of 10.82 W at 3.754  $\mu\text{m}$  with the conversion efficiency of 13.68%. The corresponding total output power reaches 35.4 W.

## 1. Introduction

The high-power mid-infrared (MIR) laser sources have important applications in laser spectroscopy, atmosphere monitoring, photoelectric detection, and remote sensing surveys [1–5]. In these applications, optical parametric oscillators (OPOs) based on MgO-doped periodically poled lithium niobate (MgO:PPLN) are a proven approach to realize high-power MIR lasers. In particular, MgO:PPLN OPOs pumped by Yb-doped fiber lasers (YDFLs) have the ability to convert near-infrared (NIR) radiation into MIR with high efficiency and high beam quality. Further, with their benefits of small size, light weight, and excellent heat dissipation, fiber-laser-pumped MgO:PPLN OPOs have attracted considerable research interest in recent years. In this regard, Lin et al. demonstrated a MgO:PPLN-based OPO pumped by a nanosecond-pulse linearly polarized YDFL operating at 1060 nm with the pulse duration of 20 ns at a repetition rate of 100 kHz. The OPO generated the maximum power of 5.5 W at 3.82  $\mu\text{m}$  with an optical-to-optical conversion efficiency of  $\sim 9.5\%$  [6]. Meanwhile, Liu et al. proposed a continuous-wave (CW) MgO:PPLN OPO pumped by a single-frequency linearly polarized YDFL with the output power of 49 W, and they obtained MIR output powers of 4.2 W at 3820 nm with the conversion efficiency of 8.6% [7]. Further, Liu et al. reported a tunable signal-resonant MgO:PPLN OPO pumped by a YDFL, and they obtained MIR output powers of 1.03 W and 0.67 W at 3.7  $\mu\text{m}$  and 3.9  $\mu\text{m}$  with

conversion efficiencies of 14.3% and 9.3%, respectively [8]. Shukla et al. presented a signal-resonant MgO:PPLN-based OPO pumped by a YDFL. A maximum power of 2 W was achieved at 3895 nm with optical-to-optical conversion efficiency of  $\sim 12.5\%$  [9]. Previously, we have also reported an idler-resonant miniaturized MgO:PPLN OPO pumped by an all-fiber YDFL with the thermoelectric cooling configuration. A stable maximum MIR power of 5.84 W at 3.76  $\mu\text{m}$  was obtained, the conversion efficiency was more than 14.0%, and  $M^2$  factors were 1.57 and 1.49 along the horizontal and vertical directions, respectively [10,11].

In order to improve the MIR output power, the optical parametric amplifier (OPA) was proposed to amplify the MIR laser generated by OPO. Along these lines, Parsa et al. demonstrated a picosecond YDFL-pumped idler-resonant OPO using MgO:PPLN with the MIR power of more than 400 mW across a continuous tuning range of 4028–2198 nm [12]. And then they adopted the scheme of MgO:PPLN-based cascaded optical parametric generator (OPG) and OPA, the maximum power was increased to 6.3 W near 2  $\mu\text{m}$  [13]. Later, the maximum output power of the cascaded OPG and OPA was further increased to 8.3 W [14]. Chen et al. presented the OPO and OPA scheme using two MgO:PPLN crystals pumped by a multi-channel YDFL. At a repetition frequency of 140 kHz, the maximum MIR output power of 4.69 W was obtained at 3.8  $\mu\text{m}$  with the conversion efficiency of 7.3%, and the  $M^2$  factor was 1.82 [15].

However, in all these approaches, the output power is much lower than the MgO:PPLN OPOs pumped by solid-state lasers which obtained

\* Corresponding author.

E-mail address: [feichenny@126.com](mailto:feichenny@126.com) (F. Chen).

<https://doi.org/10.1016/j.optlastec.2021.107545>

Received 10 June 2021; Received in revised form 24 August 2021; Accepted 14 September 2021

Available online 11 October 2021

0030-3992/© 2021 Elsevier Ltd. All rights reserved.

output power of 22.6 W at 3.86  $\mu\text{m}$  [16]. The main reason is that the output power of linearly polarized YDFL is relatively low, especially the pulse linearly polarized YDFL with high peak power, which can make OPO have high conversion efficiency and stability easily. With the rapid development of fiber lasers, pulse linearly polarized YDFL is easy to achieve high power laser output with low cost. In the case of high-power YDFL pumping, MgO:PPLN OPO can also achieve high-power MIR laser, and the structure is simpler than OPA scheme.

Against this backdrop, in this paper, we report on a high-power MgO:PPLN OPO operating at  $\sim 3.8\text{ }\mu\text{m}$ . The pump source is a high-power linearly polarized pulse all-fiber YDFL using master oscillator power amplifier (MOPA) structure. The performance of the all-fiber YDFL is firstly researched and its maximum power reaches  $79.1\text{ W}$  at  $1064.1\text{ nm}$ . Subsequent experiments are carried out to explore how the output power of the OPO is influenced by the repetition rate, pulse width, and waist diameter of the YDFL. Via optimization of above parameters, our OPO achieves a maximum MIR power of  $10.82\text{ W}$  at  $3.754\text{ }\mu\text{m}$  with a conversion efficiency of  $13.68\%$ . To the best of our knowledge, this is the highest MIR power above  $3.7\text{ }\mu\text{m}$  reported thus far with the use of the fiber-laser-pumped MgO:PPLN-based OPO configuration. The corresponding total output power of the OPO is  $35.4\text{ W}$  with a conversion efficiency of  $44.75\%$ .

## 2. Experimental setup

The OPO based on MgO:PPLN consists of a linearly polarized all-fiber YDFL module and an OPO module. The linearly polarized all-fiber YDFL module generates a pump laser. Based on the MOPA structure, the YDFL includes the master-oscillation and power-amplifier stages, as shown in Fig. 1. The master-oscillation stage comprises a linearly polarized distributed feedback (DFB) laser utilized to produce the seed laser at 1064 nm. The output power of the DFB laser is controlled by a rectangular modulated signal from a signal generator (33500B, Agilent). By adjusting the modulated signal, the repetition rate and pulse width of seed laser can be set, thus the repetition rate and pulse width of YDFL can be controlled. The power amplifier stage comprises three-stage linearly polarized Yb-doped fiber amplifiers (YDFAs) pumped by 976-nm laser diodes (LDs). All YDFAs are forwardly pumped and use the polarization-maintaining (PM) Yb-doped fiber (YDF) as the gain medium. The first stage YDFA adopts PM YDF with core diameter of 6  $\mu\text{m}$ , and the output power is  $\sim 100$  mW. Both the second and third YDFAs use double-cladding PM YDF with the core diameter of 12  $\mu\text{m}$  and 30  $\mu\text{m}$ , respectively. The output power of the second YDFA is  $\sim 2$  W. And the

output power of the third amplifier can be adjusted by the LD power. The PM YDF is coiled to improve the beam quality of the fiber laser and reduce the module size. In front of every YDFA, there are PM isolators (ISOs) to prevent backward laser. The amplified fiber laser outputs through the PM fiber collimator.

The schematic of OPO module is shown in Fig. 2. The pump laser firstly goes through the Faraday ISO which can protect the YDFL module from any unwanted reflections. Meanwhile, the pump polarization is rotated to the vertical direction to align along the principal axis of the MgO:PPLN crystal for maximum OPO conversion efficiency. Subsequently, the pump beam diameter is reduced in size by the lens group which comprised a plano-convex len M1 and a plano-concave len M2. By choosing different combinations of focal-length lenses, we can set the diameter of the pump beam waist to required values. Next, the fiber laser is coupled into the MgO:PPLN crystal. The dimensions of the MgO:PPLN crystal are  $50\text{ mm} \times 3\text{ mm} \times 2\text{ mm}$ , and the grating period is  $29.5\text{ }\mu\text{m}$ . Both ends of the MgO:PPLN crystal are antireflection-coated for wavelengths of  $1.06\text{ }\mu\text{m}$ ,  $1.48\text{ }\mu\text{m}$ , and  $3.8\text{ }\mu\text{m}$ . The crystal is placed in a temperature control oven operating at  $70\text{ }^{\circ}\text{C}$  with a precision of  $\pm 0.1\text{ }^{\circ}\text{C}$ . The resonant cavity consists of a flat input mirror M3 and a flat output coupler M4. The signal-resonant and pump-double-pass scheme is used to achieve high optical-to-optical conversion efficiency. Therefore, M3 is antireflection-coated at  $1.06\text{ }\mu\text{m}$  and high-reflection-coated at  $1.48\text{ }\mu\text{m}$  and  $3.8\text{ }\mu\text{m}$ . M4 is high-reflection-coated at  $1.06\text{ }\mu\text{m}$ , antireflection-coated at  $3.8\text{ }\mu\text{m}$  and for  $\sim 70\%$  reflection at  $1.48\text{ }\mu\text{m}$ . The length of the resonant cavity is  $80\text{ mm}$  the MgO:PPLN crystal is in the center of the cavity. The OPO process occurs due to the feedback effect of the resonant cavity, which affords the NIR signal laser and the MIR idler laser output. A dichroic mirror M5 can be used to filter out the signal and achieve the MIR laser output.

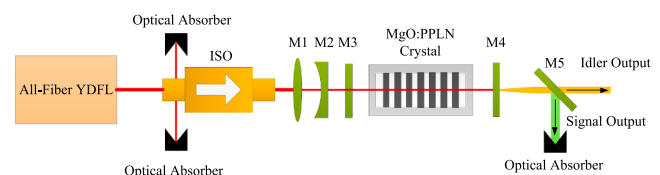


**Fig. 2.** Schematic of OPO module based on MgO:PPLN.

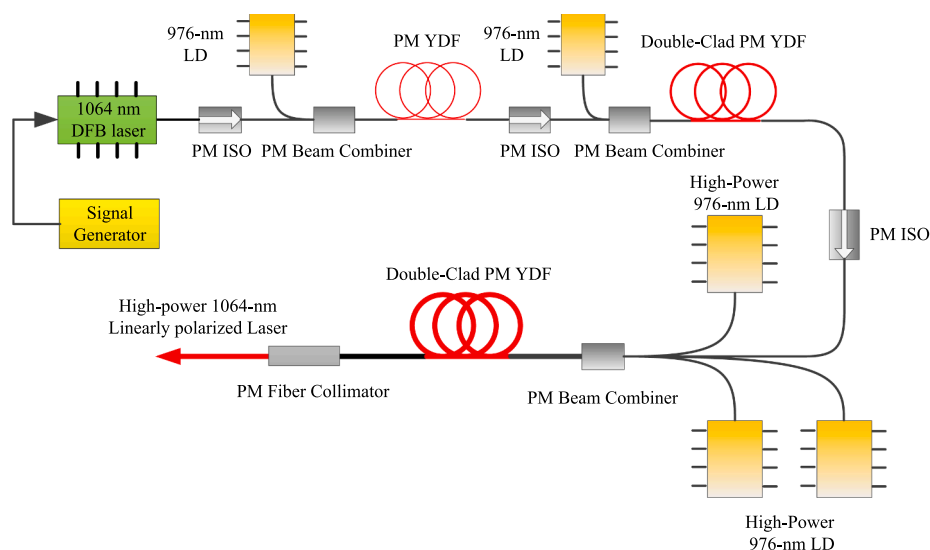


**Fig. 1.** Schematic of linearly polarized all-fiber YDFL module.

### 3. Results and discussion

#### 3.1. Characteristics of all-fiber YDFL

In our study, we firstly investigate the output power of the all-fiber YDFL for different repetition rates and pulse widths. The modulated signal repetition rate is varied as 200 kHz, 250 kHz, and 300 kHz and the modulated signal pulse width is 200 ns. We measure the average output power of the YDFL after the Faraday ISO and the results are depicted in Fig. 3(a). It can be observed that the output power of the YDFL is almost same for different repetition rates. However, with the LD power increasing, higher repetition rates corresponds to larger stable output powers. The maximum stable output power of YDFL is 60.3 W, 70.6 W and 79.1 W at 200 kHz, 250 kHz and 300 kHz, respectively. Similarly, when the repetition rate is 300 kHz and the modulated signal pulse width is varied as 150 ns, 175 ns, and 200 ns, Fig. 3(b) shows the average output power of the YDFL (after the Faraday ISO) as functions of the third stage LD power. The results show that the fiber laser power is almost unaffected by pulse width. But when the LD power becomes high, larger pulse width is conducive to higher stable output power. With the pulse width of 150 ns, 175 ns and 200 ns, the maximum stable output power of YDFL is 58.4 W, 64.8 W and 79.1 W, respectively. The main reason for this is that when the output power is equal, a lower repetition rate or pulse width leads to higher pulse peak power, which is easy to induce nonlinear effect in fiber and make YDFL unstable.

When the modulated signal repetition rate and pulse width are 300 kHz and 200 ns, respectively, the temporal waveforms of the seed and YDFL output laser are measured by using the NIR photoelectric detector (APD110C/M, Thorlabs) and the oscilloscope (DSO-X 4104A, Keysight). As shown in Fig. 4(a), we can observe that the waveform of the seed is similar to the rectangular modulated signal. But for the YDFL output laser, the intensity of the pulse leading edge is stronger than the pulse trailing edge. Because in the amplification process, the gain of the pulse leading edge is higher than the pulse trailing edge. With the maximum output power, the spectrum and beam profile of the YDFL are shown in Fig. 4(b), the central wavelength of the YDFL is 1064.1 nm and the full-width at half-maximum (FWHM) line width is  $\sim 1.7$  nm. The corresponding  $M^2$  factors along the horizontal and vertical directions are 1.26 and 1.22, respectively.

#### 3.2. Characteristics of OPO and optimization

##### 3.2.1. Influence of repetition rate

As a next step, the characteristics of the MgO:PPLN OPO pumped by the all-fiber YDFL is investigated in our experiments. We ensure that the pump beam waist lies at the center of the MgO:PPLN crystal, and the beam waist diameter is  $\sim 230$   $\mu\text{m}$ . The length of the cavity is set to 80 mm. The dependence of the output power of the OPO on the repetition

rate is firstly researched. Upon fixing modulated signal pulse width as 200 ns, we vary repetition rate as 200 kHz, 250 kHz, and 300 kHz. The MIR idler power and the total power of signal and idler are measured and the results are summarized in Fig. 5. We observe that when the pump power is less than 50 W, the idler power and total power increase slightly with the decrease of repetition rate. This is because lower repetition rate corresponds to larger pump pulse peak power, which can improve the optical-to-optical conversion efficiency in the case of lower pump power. But when the pump power exceeds 50 W, the idler power and total power improve a little as repetition rate increases. With the pump power of  $\sim 60$  W, the MIR power reach 7.75 W at 200 kHz, 8.15 W at 250 kHz and 8.40 W at 300 kHz, and the corresponding total power is 26.6 W, 27.5 W, and 28.2 W, respectively. This result suggests that with the high pump power, the MgO:PPLN crystal generates strong temperature gradients due to the idler absorption, which affects the phase matching conditions and reduces the optical-to-optical conversion efficiency [6]. And larger pump power density will aggravate the temperature gradients and result in a lower output power with the lower repetition rate.

The waveforms can also exhibit the influence of pump intensity on output power. We use the NIR and MIR photoelectric detector (PV-2TE-4, Vigo) to measure the pump (before the OPO) and the idler waveforms, respectively. When the average pump power is  $\sim 60$  W, Fig. 6 presents the waveforms of the pump and idler operating at 200 kHz, 250 kHz, and 300 kHz. We find that with the pump pulse intensity increasing, the idler pulse becomes more and more sharp, which is similar to the phenomenon found in the signal waveforms of reference [6]. In the pulse leading edge, with the rapid increase of pump intensity, the idler intensity also grows quickly. After the peak, the idler intensity decreases with the falling pump intensity and the stronger pump intensity will accelerate the decrease of idler intensity. As a result, when reaching the pulse trailing edge, the idler intensity at 200 kHz has little difference compared with the ones at 250 kHz and 300 kHz. Therefore, when the pump power density is high, not only the conversion efficiency near the pulse trailing edge will be reduced, but also the MIR pulse width will be narrowed. At 200 kHz, 250 kHz, and 300 kHz, the idler FWHM pulse duration is 76.8 ns, 98.4 ns, and 118.4 ns, respectively.

##### 3.2.2. Influence of pulse width

The pulse width of the modulated signal also influences the OPO output power. To investigate this aspect, we set the repetition rate to be 300 kHz and the modulated signal pulse width is chosen as 150 ns, 175 ns, and 200 ns. The other experimental conditions are the same as the previous case. The dependence of the idler power and total power on the pump power is depicted in Fig. 7. Similar to Fig. 5, Fig. 7 shows that when the pump power is less than 50 W, the idler power and total power with smaller pulse width is higher. However, with the pump power exceeding 50 W, due to the higher pulse peak power with smaller pulse

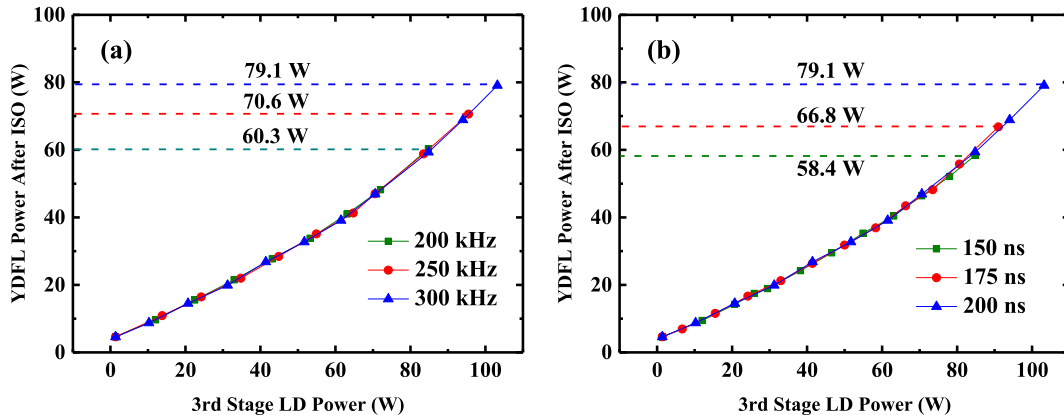


Fig. 3. Average output power of YDFL versus third stage LD power for different (a) repetition rates and (b) pulse widths.

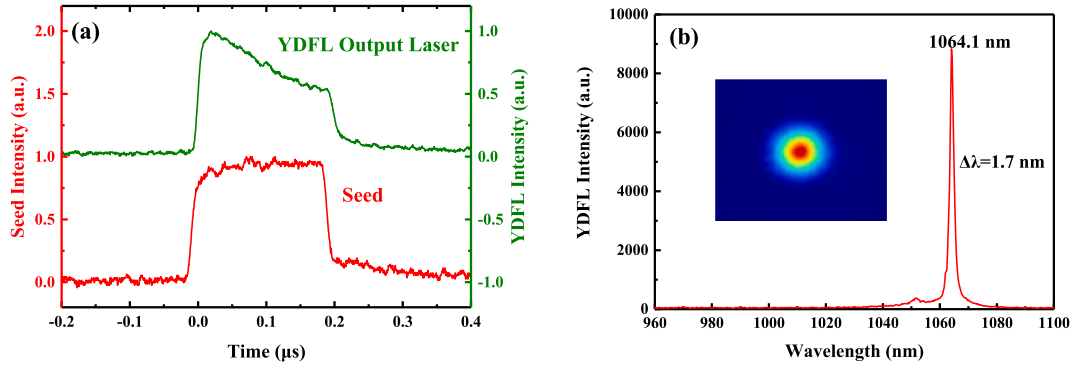


Fig. 4. (a) Waveforms of seed and YDFL output laser operating at 300 kHz with modulated signal pulse width of 200 ns; (b) spectrum and beam profile of YDFL with maximum output power.

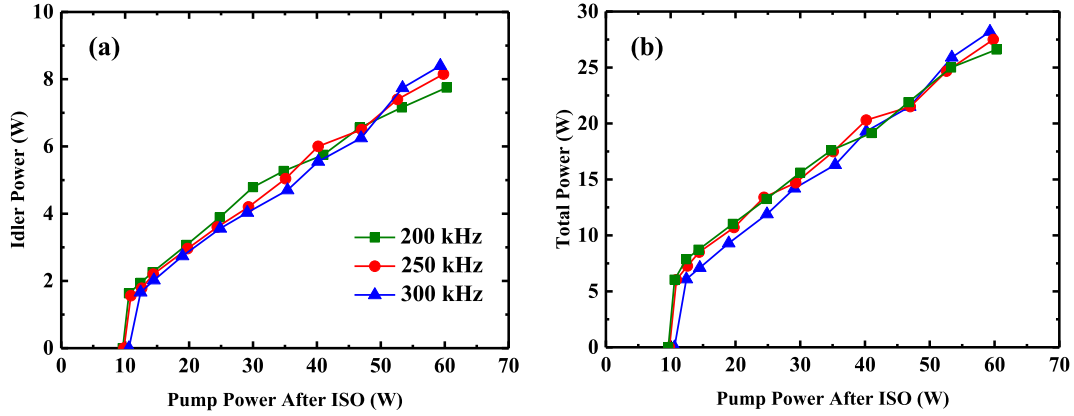


Fig. 5. (a) Idler and (b) total output power of OPO as functions of pump power after ISO for different repetition rates.

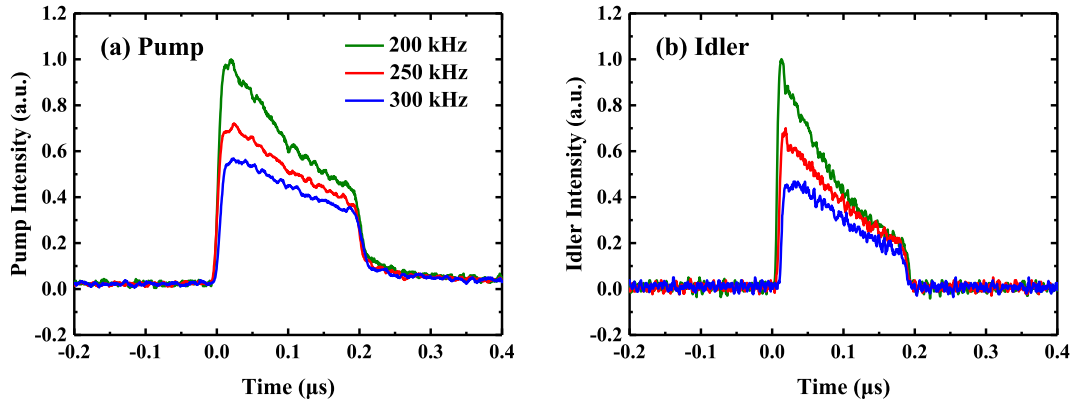


Fig. 6. Waveforms of (a) pump and (b) idler with pump power of ~60 W for different repetition rates.

width, the temperature gradients become more serious so that the idler power and total power become lower. For the pulse width of 150 ns, 175 ns, and 200 ns, the idler power is 7.86 W, 8.12 W, and 8.40 W, respectively. The corresponding total power is 26.5 W, 27.2 W, and 28.2 W, severally.

When the average pump power is ~60 W, Fig. 8 displays the pump and idler waveforms with the modulated signal pulse width of 150 ns, 175 ns, and 200 ns. We can also observe that with the pump pulse intensity increasing, the idler intensity in the pulse leading edge becomes higher, but the intensity of the pulse trailing edge is almost constant. For the pulse width of 150 ns, 175 ns, and 200 ns, the idler FWHM pulse duration is 89.6 ns, 99.6 ns, and 118.4 ns, respectively.

### 3.2.3. Influence of diameter of pump waist

The dependence of the OPO output power on the diameter of the pump waist is also investigated. The modulated signal repetition rate and pulse width are 300 kHz and 200 ns, respectively. In order to suppress the temperature gradients, we expand the waist diameter to ~340 μm to reduce the pump power density. With other experimental conditions remaining unchanged, the results are summarized in Fig. 9. We observe that the output power declines and the pump threshold raises with the increase of waist diameter. Compared with 230-μm waist, the maximum idler power and total power with 340-μm waist reduce to 7.92 W and 25.7 W, respectively. And the pump threshold rises to ~20 W. The above results indicate that when the pump waist diameter is 340 μm, the pump power density is too low to obtain high conversion

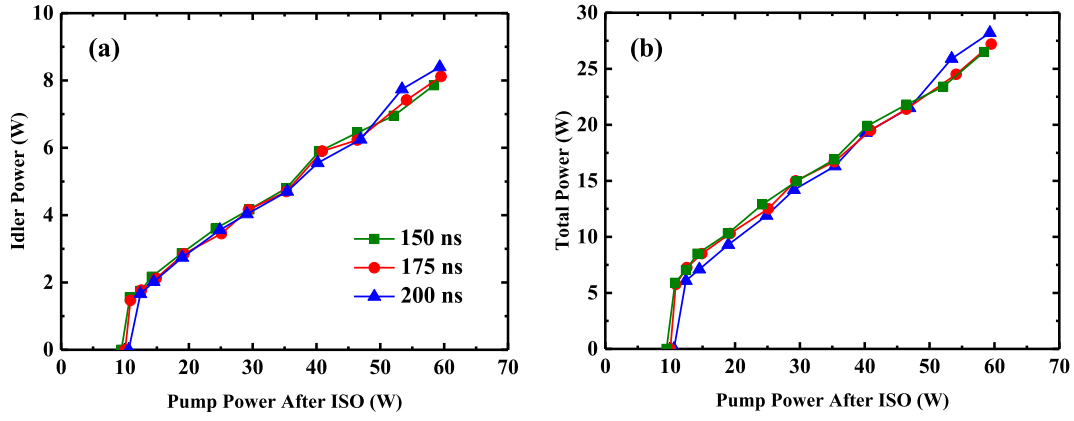


Fig. 7. (a) Idler and (b) total output power of OPO as functions of pump power after ISO for different pulse widths.

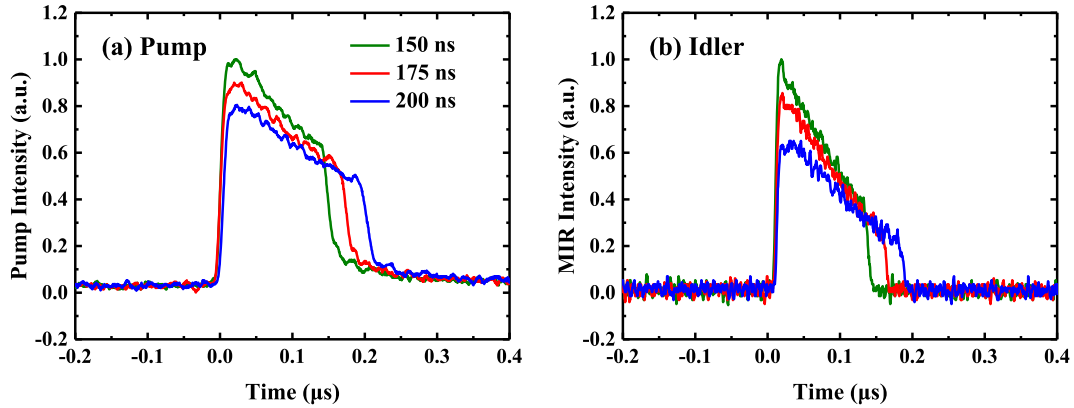


Fig. 8. Waveforms of (a) pump and (b) idler with pump power of  $\sim 60$  W for different pulse widths.

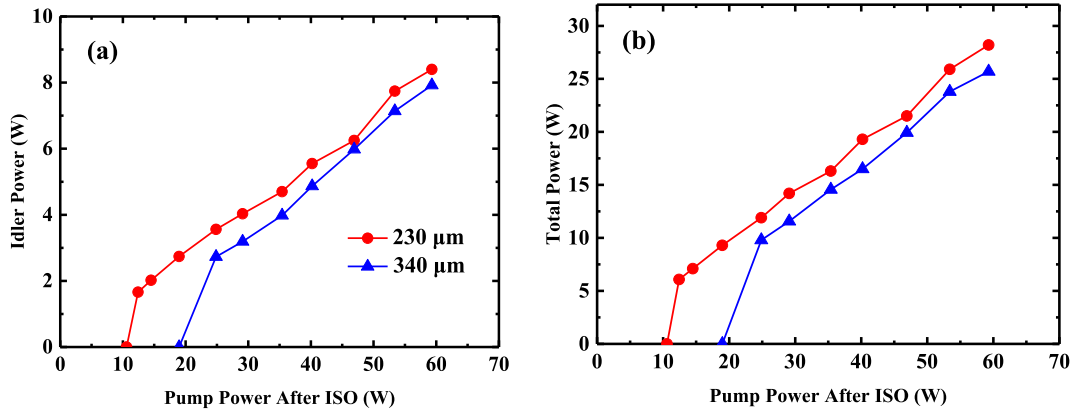


Fig. 9. (a) Idler and (b) total output power of OPO as functions of pump power after ISO for different pump waist diameters.

efficiency.

### 3.2.4. Power scaling

The abovementioned results indicate that the output power is optimal when pump repetition rate, pulse width, and waist diameter are 300 kHz, 200 ns, and 230  $\mu$ m, respectively. And when operating at 300 kHz with the pulse width of 200 ns, the YDFL can output high-power stable pump laser. Therefore, we continue to improve the pump power and measure the output performance of the OPO. Fig. 10 depicts the idler power and total power as functions of the pump power (increased up to 79.1 W) for the abovementioned settings. When the pump power is more than 60 W, the output power still increases with the pump power.

The idler and total optical-to-optical conversion efficiencies maintain above 13% and 44%, respectively. The maximum MIR power can reach 10.82 W and the relevant optical-to-optical conversion efficiency is 13.68%. The maximum total power of 35.4 W is achieved with a conversion efficiency of 44.75%. The maximum electric power consumption of the whole fiber-laser-pumped OPO system is 277 W and the wall-plug efficiencies of idler and total output laser are 3.91% and 12.78%, respectively.

Fig. 11(a) and (b) show the pump waveforms (before the OPO) for different powers and the corresponding idler waveforms, respectively. Obviously, in the pulse trailing edge, when the pump power less than 40.2 W, the idler intensity increases with the pump intensity. However,

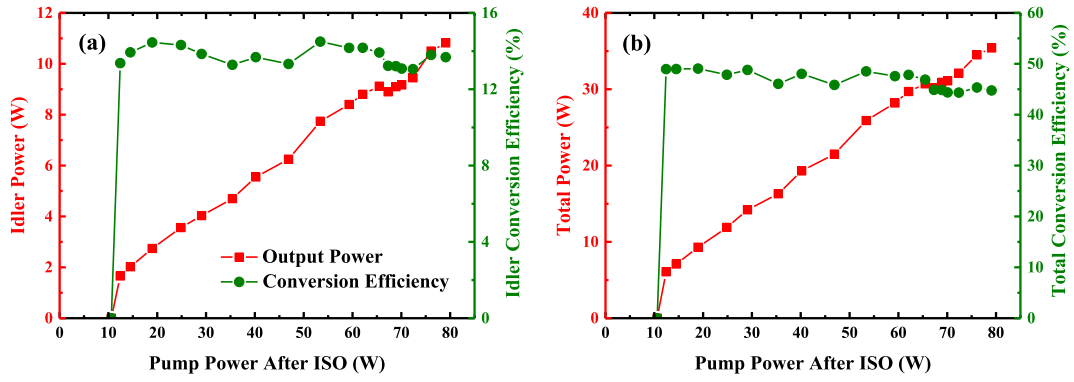


**Fig. 10.** (a) Idler and (b) total output power of OPO as functions of pump power after ISO when pump repetition rate, pulse width, and waist diameter are 300 kHz, 200 ns, and 230  $\mu\text{m}$ , respectively.

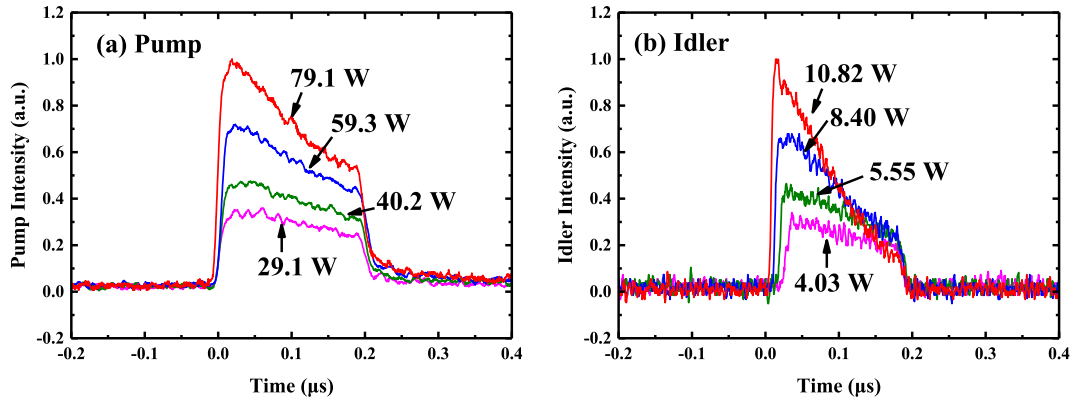


**Fig. 11.** (a) Pump and (b) idler waveforms for different powers.

for the pump power of 59.3 W, the idler intensity of the pulse trailing edge improves barely. When the pump power achieves 79.1 W, the idler intensity of the pulse trailing edge even begin to decline. But because of the rising idler intensity of the pulse leading edge, the average idler power still increases with the pump power. When the pump pulse energy is high, the decrease of idler conversion efficiency in the pulse trailing edge maybe related to the thermal effect in the MgO:PPLN crystal, and the specific reason needs to be analyzed theoretically or experimentally in the future research.

At full output power, the MIR spectrum and  $M^2$  factors are measured by the spectrometer (FT-MIR 2–6  $\mu\text{m}$ , Arcoptix) and the camera (Win-cam-IR-BB, Dataray), respectively. As shown in Fig. 12(a), the idler central wavelength is 3.754  $\mu\text{m}$  and the FWHM line width is less than 17 nm. In Fig. 12(b), the  $M^2$  factors of the idler along the horizontal and

vertical directions are 2.98 and 2.08, respectively.

#### 4. Conclusion

In our study, we propose a linearly polarized all-fiber YDFL-pumped OPO based on MgO:PPLN. Firstly, we present the MOPA scheme of the linearly polarized all-fiber YDFL and analyze the output characteristics. Subsequently, we experimentally investigate the OPO characteristics as functions of pump repetition rate, pulse width, and waist diameter. Our results indicate that if the pump power density is too high, not only the optical-to-optical conversion efficiency will reduce, but also the idler FWHM pulse width will become narrow. The experiments also prove that the low pump power density can't guarantee the high output power and conversion efficiency of the OPO. By adjusting the pump repetition

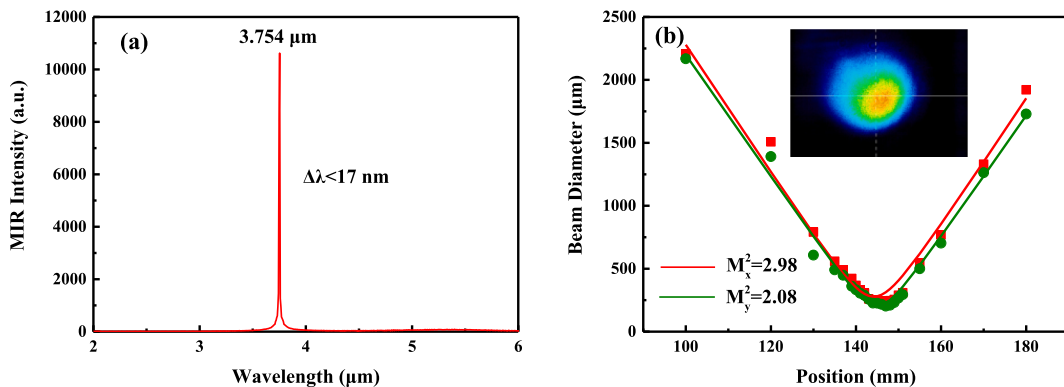


**Fig. 12.** (a) Spectrum and (b)  $M^2$  factors of idler at full output power.



rate, pulse width, and waist diameter, the appropriate pump power density can be obtained. Via optimizing, when we set repetition rate, pulse width, and waist diameter as 300 kHz, 200 ns, and 230  $\mu\text{m}$ , respectively, the OPO can achieve a maximum MIR power of 10.82 W at 3.754  $\mu\text{m}$  with a conversion efficiency of 13.68%. To the best of our knowledge, this is the highest MIR power above 3.7  $\mu\text{m}$  reported thus far with the use of the fiber-laser-pumped MgO:PPLN-based OPO configuration. The corresponding  $M^2$  factors of the idler along the horizontal and vertical directions are 2.98 and 2.08, respectively. The maximum total power of OPO reaches 35.4 W with a conversion efficiency of 44.75%. In conclusion, we believe that our experimental results will be useful in designing high-power MgO:PPLN-based OPO systems pumped by all-fiber YDFLs with high conversion efficiency.

### Declaration of Competing Interest

The authors declare that they have no known competing financial interests or personal relationships that could have appeared to influence the work reported in this paper.

### Acknowledgements

The authors want to acknowledge the support provided by ‘National Key R&D Program of China’ (Grant No.2018YFE0203203), ‘National Natural Science Foundation of China’ (Grant No. 62005274, Grant No.61975203), ‘Open Fund Project of the State Key Laboratory of Laser Interaction with Matter’ (Grant No. SKLLIM1815).

### References

- [1] M. Vlk, A. Datta, S. Alberti, H.D. Yallev, V. Mittal, G.S. Murugan, J. Jágorská, Extraordinary evanescent field confinement waveguide sensor for mid-infrared trace gas spectroscopy, *Light Sci. Appl.* 10 (26) (2021) 1–7.
- [2] M. Yan, P.L. Luo, K. Iwakuni, G. Millot, T.W. Hansch, N. Picque, Mid-infrared dual-comb spectroscopy with electro-optic modulators, *Light Sci. Appl.* 6(10) (2017) e17076.
- [3] N. Dixit, R. Mahendra, O.P. Naraniya, A.N. Kaul, A.K. Gupta, High repetition rate mid-infrared generation with singly resonant optical parametric oscillator using multi-grating periodically poled MgO:LiNbO<sub>3</sub>, *Opt. Laser Technol.* 42 (1) (2010) 18–22.
- [4] P. Weibring, H. Edner, S. Svanberg, Versatile mobile lidar system for environmental monitoring, *Appl. Opt.* 42 (18) (2003) 3583–3594.
- [5] K.P. Petrov, L. Goldberg, W.K. Burns, R.F. Curl, F.K. Tittle, Detection of CO in air by diode-pumped 4.6- $\mu\text{m}$  difference-frequency generation in quasi-phase-matched LiNbO<sub>3</sub>, *Opt. Lett.* 21 (1) (1996) 86–88.
- [6] D. Lin, S. Alam, Y. Shen, T. Chen, B. Wu, D.J. Richardson, Large aperture PPMgLN based high-power optical parametric oscillator at 3.8  $\mu\text{m}$  pumped by a nanosecond linearly polarized fiber MOPA, *Opt. Express* 20 (14) (2012) 15008–15014.
- [7] L. Liu, X. Li, H. Xiao, X.J. Xu, Z.F. Jiang, 12 W mid-infrared output, singly resonant, continuous-wave optical parametric oscillator pumped by a Yb<sup>3+</sup>-doped fiber amplifier, *Laser Phys.* 22 (1) (2012) 115–119.
- [8] S.D. Liu, Z.W. Wang, B.T. Zhang, J.L. He, J. Hou, K.J. Yang, R.H. Wang, X.M. Liu, Wildly tunable, high-efficiency MgO:PPLN mid-IR optical parametric oscillator pumped by a Yb-fiber laser, *Chin. Phys. Lett.* 31 (2) (2014), 024204.
- [9] M.K. Shukla, R. Das, High-power single-frequency source in the mid-infrared using a singly resonant optical parametric oscillator pumped by Yb-fiber laser, *IEEE J. Sel. Top. Quantum Electron.* 24 (5) (2018) 1–6.
- [10] Y. He, F. Chen, D.Y. Yu, K. Zhang, Q.K. Pan, J.J. Sun, Improved conversion efficiency and beam quality of miniaturized midinfrared idler-resonant MgO:PPLN optical parametric oscillator pumped by all-fiber laser, *Infrared Phys. Technol.* 95 (2018) 12–18.
- [11] D. Yu, Y. He, K. Zhang, Q. Pan, F. Chen, L. Guo, A tunable mid-infrared solid-state laser with a compact thermal control system, *Appl. Sci.* 8 (6) (2018) 878.
- [12] S. Parsa, S.C. Kumar, B. Nandy, M. Ebrahim-Zadeh, Yb-fiber-pumped, high-beam-quality, idler-resonant mid-infrared picosecond optical parametric oscillator, *Opt. Express* 27 (18) (2019) 25436–25444.
- [13] S.C. Kumar, B. Nandy, M. Ebrahim-Zadeh, Performance studies of high-average-power picosecond optical parametric generation and amplification in MgO:PPLN at 80 MHz, *Opt. Express* 28 (26) (2020) 39189–39201.
- [14] B. Nandy, S.C. Kumar, M. Ebrahim-Zadeh, 8.3 W average power, 80% pump depletion, picosecond mid-infrared parametric generation and amplification at 80 MHz, in *OSA High-brightness Sources and Light-driven Interactions Congress 2020* (2020) paper MTh3C.2.
- [15] B.Y. Chen, S. Wu, Y.J. Yu, C.T. Wu, Y.H. Wang, G.Y. Jin, 3.8  $\mu\text{m}$  mid-infrared optical parametric amplifier based on MgO:PPLN crystal, *Infrared Phys. Technol.* 111 (2020), 103448.
- [16] Y.F. Peng, X.B. Wei, W.M. Wang, D.M. Li, High-power 3.8  $\mu\text{m}$  tunable optical parametric oscillator based on PPMgO:CLN, *Opt. Commun.* 283 (20) (2010) 4032–4035.